



Research article

Oxidized low-density lipoprotein changes the inflammatory status and metabolomics profiles in human and mouse macrophages and microglia

Yaru Sun ^{a,b}, Jia-Jian Liang ^a, Jianming Xu ^{a,b}, Kewen Zhou ^{a,b}, Changzhen Fu ^a, Shao-Lang Chen ^a, Rucui Yang ^{a,b}, Tsz Kin Ng ^{a,c}, Qingping Liu ^{a,**}, Mingzhi Zhang ^{a,*}

^a Joint Shantou International Eye Center of Shantou University and the Chinese University of Hong Kong, Shantou, Guangdong, China

^b Shantou University Medical College, Shantou, Guangdong, China

^c Department of Ophthalmology and Visual Sciences, The Chinese University of Hong Kong, Hong Kong

ARTICLE INFO

Keywords:

Oxidized low-density lipoprotein
Macrophages
Microglia
Inflammatory response
Metabolites

ABSTRACT

The conjunctiva of primary open angle glaucoma patients showed high level of oxidized low-density lipoprotein (ox-LDL), which is associated with the inflammatory response. Microglia and macrophages are the immune cells involved in retinal ganglion cell survival regulation; yet, their roles of the ox-LDL-induced inflammation in glaucoma remain elusive. Here we aimed to investigate the lipid uptake, inflammatory cytokine expression, and metabolomics profiles of human and murine-derived microglial and macrophage cell lines treated with ox-LDL. Under the same ox-LDL concentration, macrophages exhibited higher lipid uptake and expression of pro-inflammatory cytokines as compared to microglia. The ox-LDL increased the levels of fatty acid metabolites in macrophages and sphingomyelin metabolites in microglia. In summary, this study revealed the heterogeneity in the inflammatory capacity and metabolic profiles of macrophages and microglia under the stimulation of ox-LDL.

1. Introduction

Glaucoma is a leading cause of global irreversible visual impairment and blindness, with 76.0 million people worldwide in 2020, and expected to increase to 111.8 million in 2040 [1]. Primary open-angle glaucoma (POAG), the most common form of glaucoma, is characterized by the progressive degeneration of retinal ganglion cells (RGCs) [2]. Apart from the increased intraocular pressure (IOP), inflammation has been suggested to be involved in POAG [3–5].

We previously identified the association of caveolin-1 and ATP-binding cassette transporter A1 gene variants with POAG, both of which are crucial regulators in cholesterol homeostasis [6]. We also observed that the POAG patients carrying the risk allele exhibit higher cholesterol levels [7]. Previous studies have also reported significantly higher peripheral blood LDL levels in the POAG patients as compared to the control subjects [8,9]. The elevated LDL levels can increase blood viscosity and affect the ocular microcirculation, thereby contributing to the pathogenesis of POAG [10]. The oxidized low-density lipoprotein (ox-LDL), resulted from the low-density lipoprotein (LDL) cholesterol, is present in the conjunctival specimens of the POAG patients, especially accumulated in the

* Corresponding author.

** Corresponding author.

E-mail addresses: lqp@jsiec.org (Q. Liu), zmq@jsiec.org (M. Zhang).

<https://doi.org/10.1016/j.heliyon.2024.e28806>

Received 18 January 2024; Received in revised form 22 March 2024; Accepted 25 March 2024

Available online 28 March 2024

2405-8440/© 2024 The Authors. Published by Elsevier Ltd. This is an open access article under the CC BY-NC license (<http://creativecommons.org/licenses/by-nc/4.0/>).

inflammatory cells [11]. In atherosclerosis, ox-LDL induces lipid metabolism disorders in macrophages and forms foam cells, which then release pro-inflammatory cytokines and trigger the inflammatory response [12–14]. Macrophages, derived from bone marrow hematopoietic stem cells, develop into the circulating monocytes with the stimulation by the macrophage colony-stimulating factor [15]. Under the disease conditions, macrophages breach the blood-retinal barrier by releasing inflammatory mediators that target the vascular endothelial cells [16–18]. Previous studies have shown that the monocytes/macrophages transendothelially migrate and aggregate at the optic nerve head (ONH), which could contribute to the early glaucomatous damage [5,19]. The numbers of macrophages increase in the ONH of the patients with both mild and severe glaucomatous optic neuropathy [20]. In addition, the internal limiting membrane macrophages are also involved in the nerve fiber layer phagocytosis in the areas with active glaucoma [21]. Microglia are the resident immune cells resided in the retina, derived from yolk sac progenitor cells. With the inflammatory stimulation, microglia increase in number, alter their morphology to remove cell debris by phagocytosis, and release a range of inflammatory mediators [16,22,23]. Previous studies have shown that microglia increase in numbers and become activated in glaucoma patients and animal models of glaucoma [24]. Nevertheless, the precise involvement of macrophages and microglia in the development of ox-LDL-induced inflammation in glaucoma remains insufficiently investigated.

Metabolomics characterizes the end products of cellular regulatory pathways, providing insights on how cells respond to the environmental changes [25]. Cell metabolism is able to determine the cell function [26,27]. Metabolic regulation of immune cells is of high importance as metabolic reprogramming drives both proinflammatory and anti-inflammatory processes [28–30]. Here, in this study, we aimed to investigate the changes in the phagocytosis, inflammatory capacity, and metabolomics profiles of both murine and human microglia and macrophages under the treatment of ox-LDL *in vitro*.

2. Results

2.1. Effect of ox-LDL on the viability of macrophages and microglia

We first determined the cytotoxicity of ox-LDL in macrophages and microglia. The cell viability of murine J774A.1 macrophage cells treated with 25 µg/mL and 50 µg/mL ox-LDL for 48 h decreased by 24.4% ($P = 0.006$) and 63.1% ($P < 0.0001$) respectively as compared to that before treatment (Fig. 1A). In contrast, the cell viability of BV2 microglial cells treated with 50 µg/mL ox-LDL for 48 h only decreased by 14.5% ($P < 0.0001$). Similar trends were observed in human cells. Treatment with 50 µg/mL ox-LDL for 48 h decreased the viability of THP-1 macrophages by 55.4% ($P < 0.0001$), whereas only 100 µg/mL of ox-LDL would decrease the viability of HMC3 cells by 9.7% ($P = 0.0030$). Consistently, under the same ox-LDL concentration treatment (25 µg/mL), macrophages (J774A.1 and THP-1 cells) showed a significant decrease in cell viability at 48 h, whereas microglia did not (Fig. 1B). Our results suggested that ox-LDL induces macrophage death at a lower concentration than the microglia.

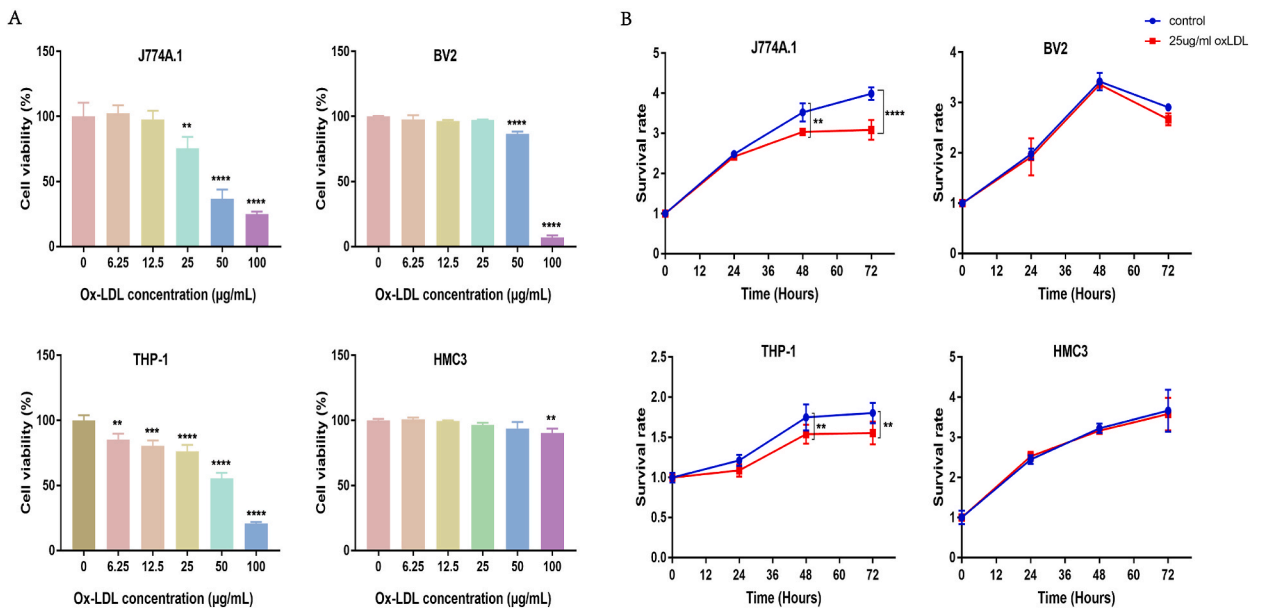


Fig. 1. Effect of ox-LDL on the viability of macrophage and microglia cell lines. (A) Changes in macrophage and microglial cell viability after treatment with 0, 6.25, 12.5, 25, 50 and 100 µg/mL ox-LDL for 48 h. (B) Changes in macrophage and microglial survival rate after treatment with 0 and 25 µg/mL ox-LDL for 0, 24, 48, and 72 h. Data presented are mean ± SD. ** $P < 0.01$, *** $P < 0.001$, **** $P < 0.0001$.

2.2. Effect of ox-LDL on lipid phagocytosis in macrophages and microglia

To assess the lipid uptake of macrophages and microglia, the intracellular lipid accumulation was evaluated by the oil red O staining. Both microglia (BV2 (79.24 ± 35.5 vs 5.715 ± 3.956, $P < 0.0001$) and HMC3 cells (44.81 ± 29.19 vs 9.727 ± 10.41, $P = 0.0112$)) and macrophages (J774A.1 (263.5 ± 103.2 vs 13.67 ± 8.307, $P < 0.0001$) and THP-1 cells (1352 ± 240.9 vs 302.7 ± 72.46, $P < 0.0001$)), under the ox-LDL treatment, showed significantly higher intensity of oil red O staining as compared to their respective control groups (Fig. 2A and B). Notably, the intensities of oil red O staining in macrophages were much higher than that in microglia.

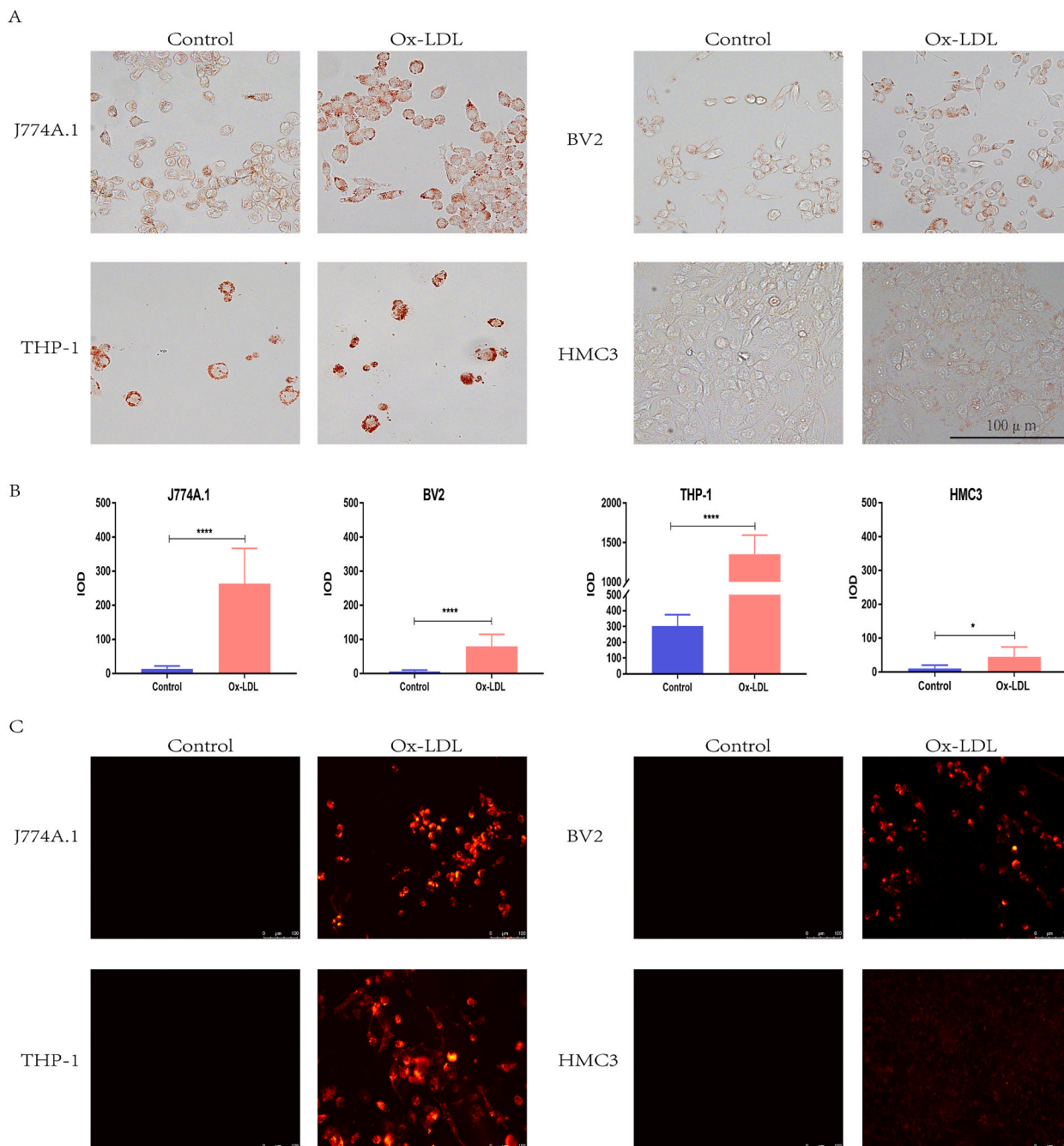


Fig. 2. Lipid accumulation in control and cells after treatment with 25 µg/mL ox-LDL for 48 h are stained by Oil Red (200 ×). (A) Lipids were stained with oil red O and examined by microscopy. (B) Quantification for foam cell. Intensity measured as integrated optical density refers to the degree of lipid accumulation. (C) DiI-ox-LDL uptake. Data presented are mean ± SD. * $P < 0.05$, **** $P < 0.0001$. (For interpretation of the references to colour in this figure legend, the reader is referred to the Web version of this article.)

Similarly, both microglia (BV2 and HMC3 cells) and macrophages (J774A.1 and THP-1 cells), under the ox-LDL treatment, showed significantly greater number of DiI-ox-LDL-positive cells as compared to their respective control groups (Fig. 2C). J774A.1 and THP-1 macrophages exhibited higher intensity of DiI-ox-LDL than the BV2 and HMC3 microglia. Collectively, our results suggested that macrophages are more likely to uptake lipids than microglia upon the ox-LDL treatment.

2.3. Effect of ox-LDL on inflammatory cytokine expression in macrophages and microglia

The expression pattern of inflammatory cytokines in ox-LDL-treated cells was determined by the qPCR analysis. Significant upregulation of tumor necrosis factor- α (TNF- α) and downregulation of interleukin-10 (IL-10) were found in J774A.1 and THP-1 macrophages treated with ox-LDL as compared to the control group (Fig. 3). In addition, THP-1 cells treated with ox-LDL also showed significant downregulation of transforming growth factor-beta (TGF- β) as compared to the control group. No significant differences were observed in the expression of inflammatory cytokine genes in the ox-LDL-treated microglial cell lines as compared to the control group. Our results indicated that ox-LDL promotes the pro-inflammatory status of macrophages, but not microglia.

2.4. Metabolomics analysis of ox-LDL-treated macrophages and microglia

For all four cell lines, the principal component analysis (PCA) results showed a clear separation between the ox-LDL treatment and control groups, and the Orthogonal partial least squares-discriminant analysis (OPLS-DA) model was reliable and valid (table S1). Compared to the control group, the metabolic footprints of the ox-LDL treatment group changed, indicating that the metabolic path was changed under the ox-LDL treatment (Fig. 4A).

The volcano plots identified 122 differentially abundance metabolites between the ox-LDL treatment and control groups in J774A.1 cells, 24 differentially abundance metabolites in BV2 cells, 28 differentially abundance metabolites in THP-1 cells, and 17 differentially abundance metabolites in HMC3 cells (Fig. 4B). Among the differentially abundance metabolites, lipids were the most significantly altered metabolites by the ox-LDL treatment in the four cell lines, accounting for 37% in J774A.1 cells, 38% in BV2 cells, 54% in THP-1 cells, and 47% in HMC3 cells (Fig. 4C). In addition, the levels of the glucose and amino acid metabolites were also

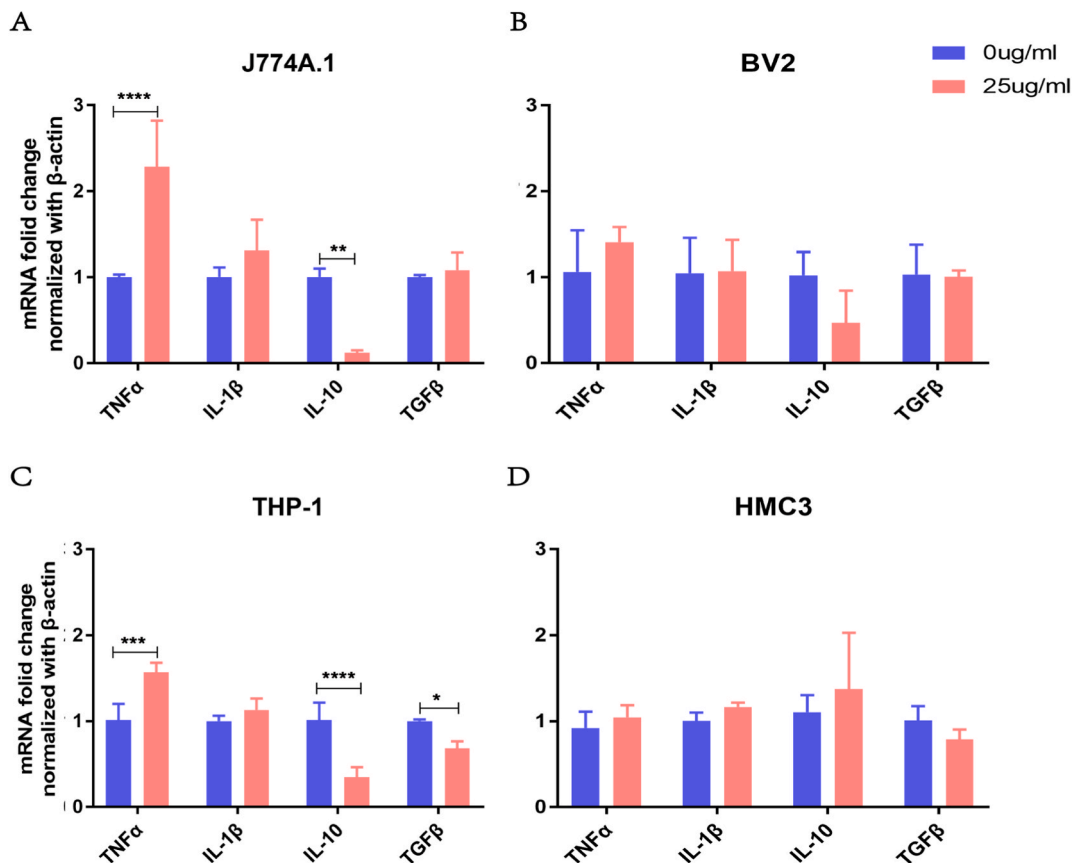


Fig. 3. Expression of inflammatory cytokines in control and cells treated with 25 μ g/mL ox-LDL for 48 h. (A) J774A.1 cell line. (B) BV2 cell line. (C) THP-1 cell line. (D) HMC3 cell line. Relative mRNA levels of indicated genes were calculated by normalizing results to β -actin. Data presented are mean \pm SD. * P < 0.05, *** P < 0.001, **** P < 0.0001.

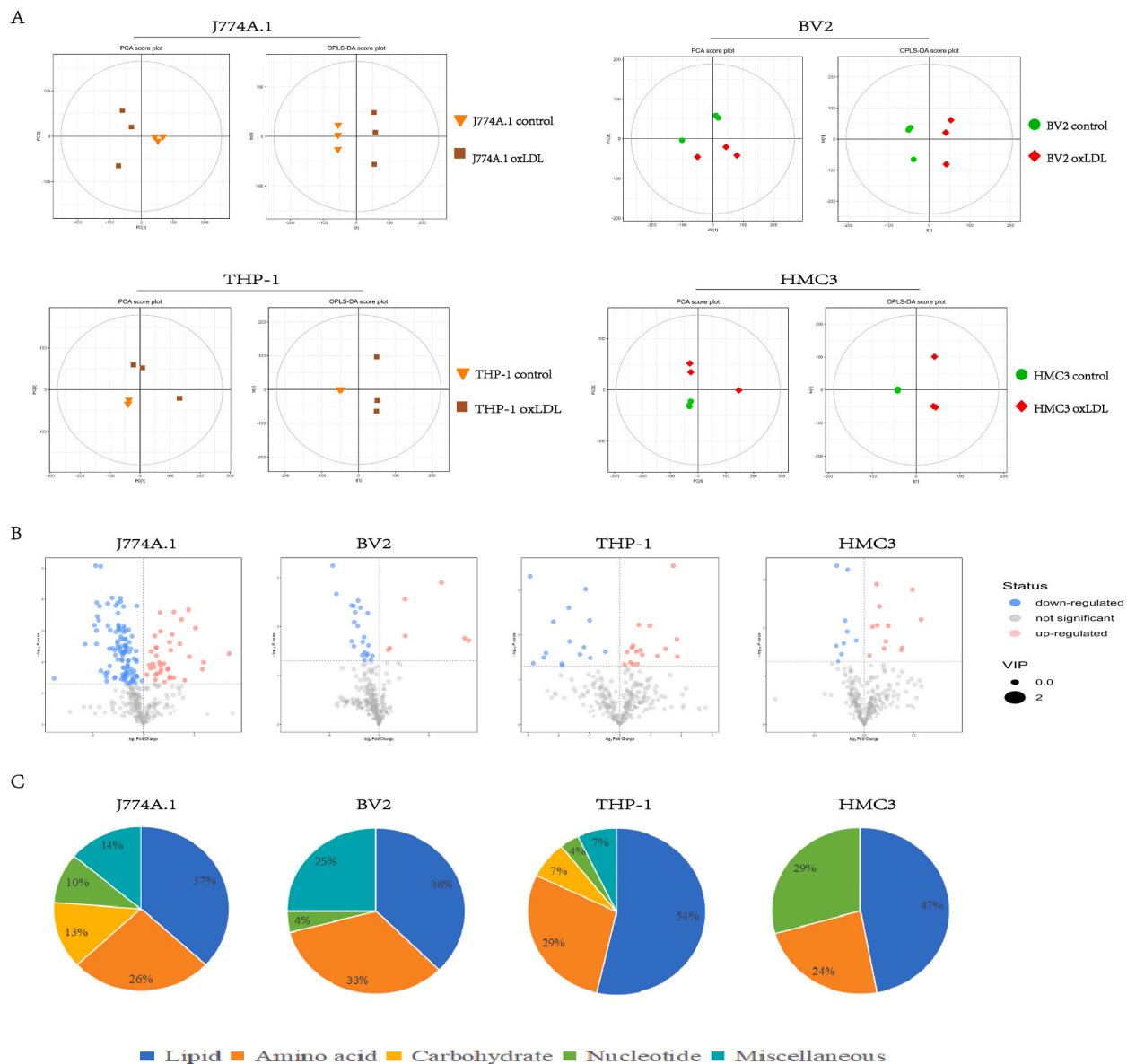


Fig. 4. Effect of ox-LDL on the metabolism of macrophage and microglia cell lines. (A) PCA plots and OPLS-DA plots of the four cell types. (B) Volcano plot analysis of differential metabolites in control and ox-LDL groups of the four cell lines. (C) Pie chart of the differential metabolite classification of the four cell lines.

substantially affected by the ox-LDL treatment (tables S2–5).

2.5. Effect of ox-LDL on lipid metabolism in macrophages and microglia

In the J774A.1 cells, the levels of long-chain carnitine metabolites and oxidized fatty acids were elevated under the treatment of ox-LDL. Similarly, ox-LDL treatment also increased the levels of fatty acid metabolites in the THP-1 cells. However, there was no significant change in the levels of long-chain carnitine metabolites in BV2 and HMC3 cells treated with ox-LDL as only two fatty acids were significantly altered (Fig. 5). In contrast, SM(d18:1/16:0) in the phospholipid metabolism increased in BV2 and HMC3 cells after ox-LDL treatment by 147.67 and 7.29 folds respectively as compared to their respective control groups (Fig. 6 and tables S3 and S5). Our findings suggested that the ox-LDL treatment increases the fatty acid metabolite levels in macrophages and sphingomyelin SM (d18:1/16:0) metabolites in microglia.

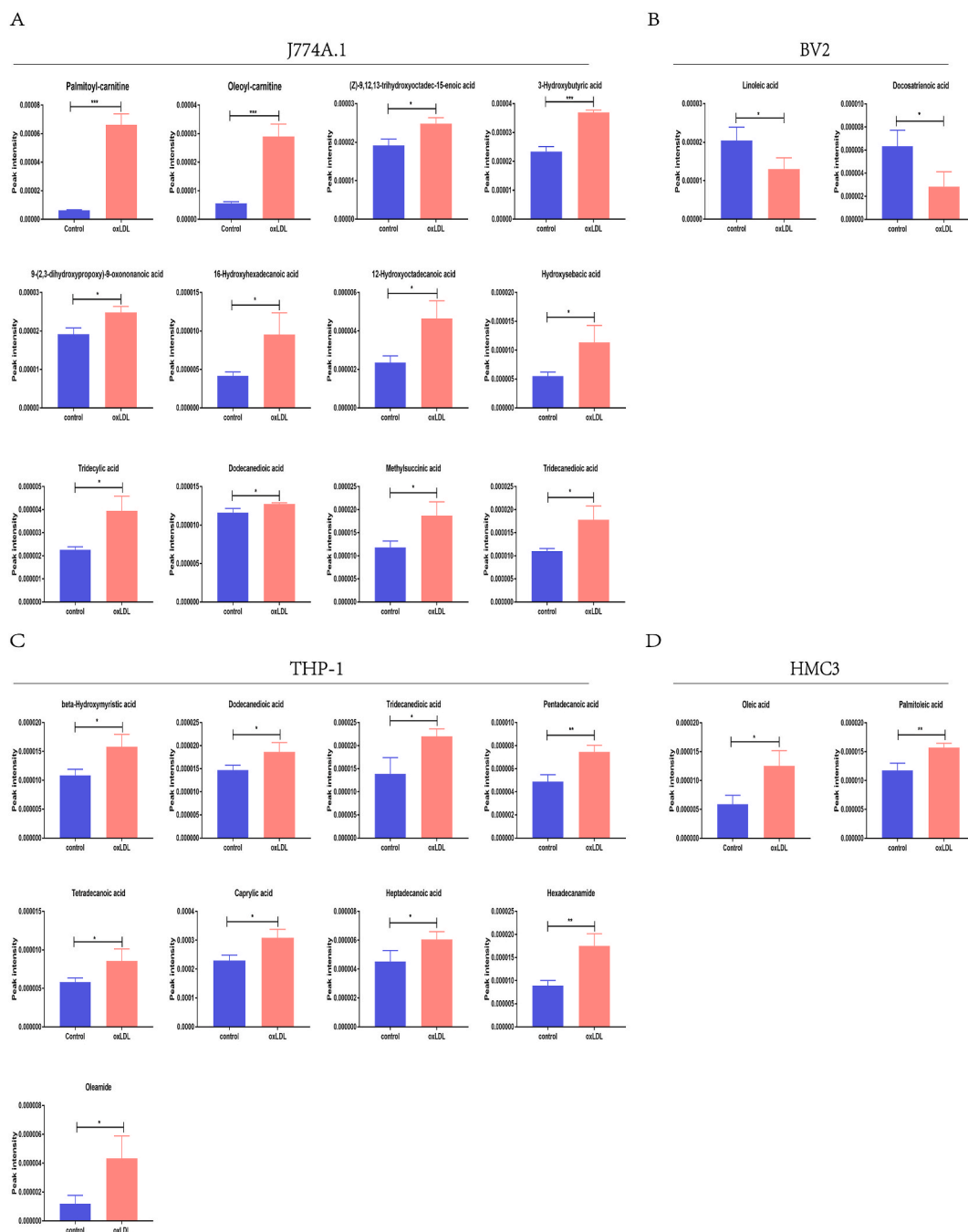


Fig. 5. Effect of ox-LDL on fatty acid metabolites of macrophage and microglia cell lines. (A) J774A.1 cell line. (B) BV2 cell line. (C) THP-1 cell line. (D) HMC3 cell line. * $P < 0.05$, ** $P < 0.01$.

2.6. Effect of ox-LDL on glucose metabolism in macrophages and microglia

In J774A.1 cells with the ox-LDL treatment, gluconic acid, fructose, phosphoenolpyruvic acid, and pyruvic acid in the glycolytic pathway, ribose 5-phosphate and erythrose 4-phosphate in the pentose phosphate pathway (PPP), and citric acid, α -ketoglutaric acid and fumaric acid in the tricarboxylic acid (TCA) cycle were decreased (Fig. 7A). In addition, maleic acid and malic acid were also decreased. In contrast, the ox-LDL treatment exhibited little effect on glucose metabolism in the THP-1, BV2, and HMC3 cells (tables S2–5). Our results indicated that J774A.1 cells show reduced glucose metabolism capacity after ox-LDL treatment.

Glucose metabolism is accompanied by energy release and consumption. Creatinine, phosphocreatine, and adenosine diphosphate (ADP) metabolites were decreased in the J774A.1 cells after the ox-LDL treatment. In the ox-LDL-treated BV2 cells, only ADP was

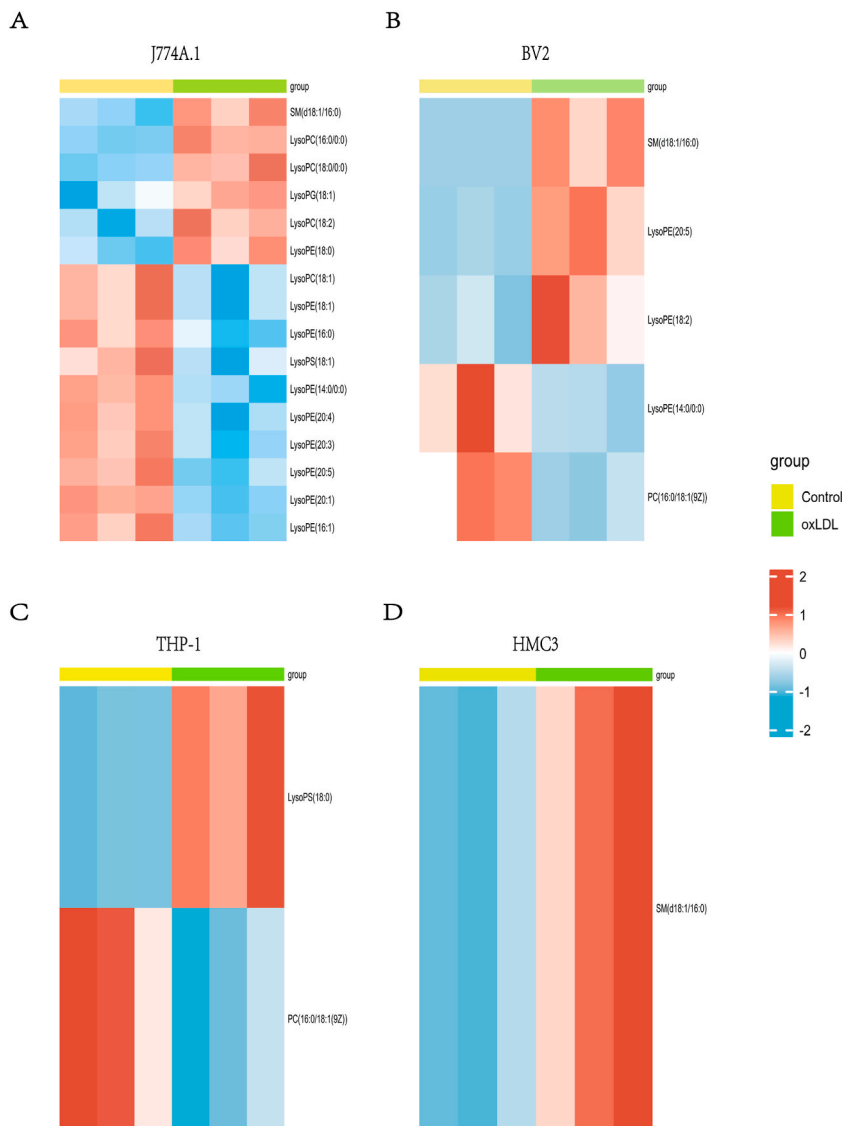


Fig. 6. Effect of ox-LDL on phospholipid metabolites of macrophage and microglia cell lines. (A) J774A.1 cell line. (B) BV2 cell line. (C) THP-1 cell line. (D) HMC3 cell line.

decreased. Instead, phosphocreatine, ADP, and adenosine triphosphate (ATP) were decreased in the ox-LDL-treated THP-1 cells. In the HMC3 cells treated with ox-LDL, only phosphocreatine metabolites were decreased (Fig. 7B). Our results suggested that the energy metabolisms in both macrophages and microglia are affected by the ox-LDL treatment.

2.7. Effect of ox-LDL on amino acid metabolism in macrophages and microglia

The glutathione (GSH) metabolism was altered in the ox-LDL-treated J774A.1 cells, with decreased glutathione, glutamic acid, cysteine, and glycine metabolites. The BV2 cells under the ox-LDL treatment also showed similar changes as the J774A.1 cells. On the contrary, glutamic acid and glycine metabolites were increased in the THP-1 cells. The GSH metabolism was not altered in the HMC3 cells.

The branched-chain amino acids are composed of valine, leucine, and isoleucine, which can be converted into pyruvic acid for energy generation. Both leucine and isoleucine metabolites were decreased in the ox-LDL-treated J774A.1 cells, and only ketoleucine, the upstream product of leucine, was decreased in the ox-LDL-treated BV2 cells. In the ox-LDL-treated THP-1 cells, the isoleucine metabolites were decreased, but leucine did not change significantly. In the HMC3 cells treated with ox-LDL, both γ -glutamyl leucine and ketoleucine were decreased. Our findings suggested that ox-LDL differentially affects the branched-chain amino acid metabolism in macrophages and microglia (Fig. 8).

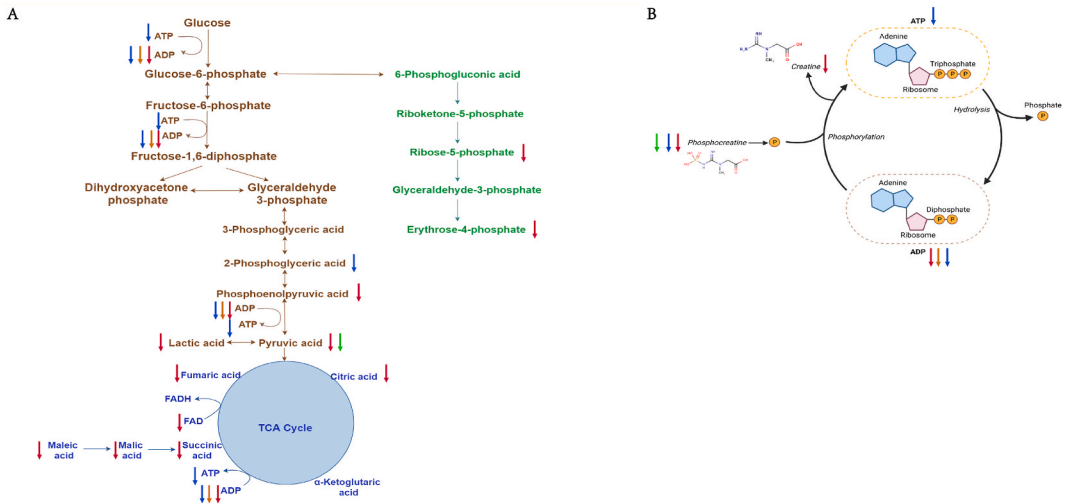


Fig. 7. Effect of ox-LDL on glucose and energy metabolism of macrophage and microglia cell lines. (A) Effect of ox-LDL on glucose metabolism. (B) Effect of ox-LDL on energy metabolism. ↓J774A.1 cells, ↓BV2 cells, ↓THP-1 cells, ↓HMC3 cells.

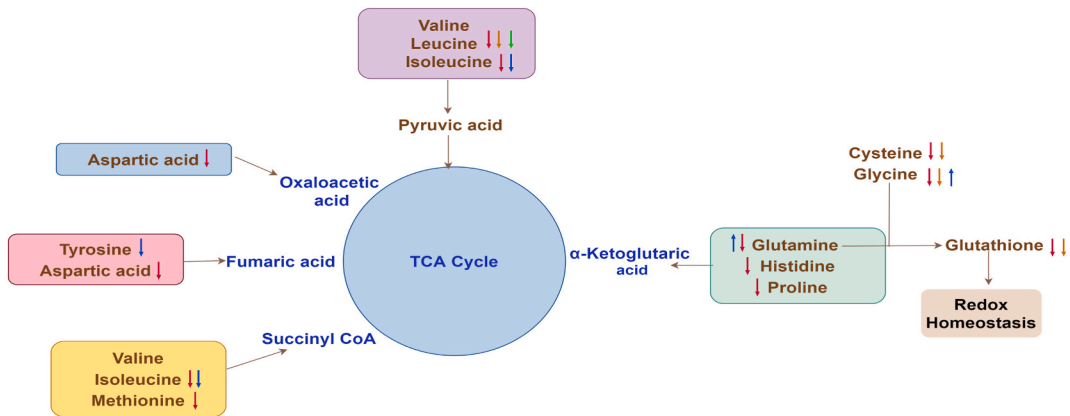


Fig. 8. Effect of ox-LDL on amino acid metabolism of macrophage and microglia cell lines. ↓J774A.1 cells, ↓BV2 cells, ↓THP-1 cells, ↓HMC3 cells.

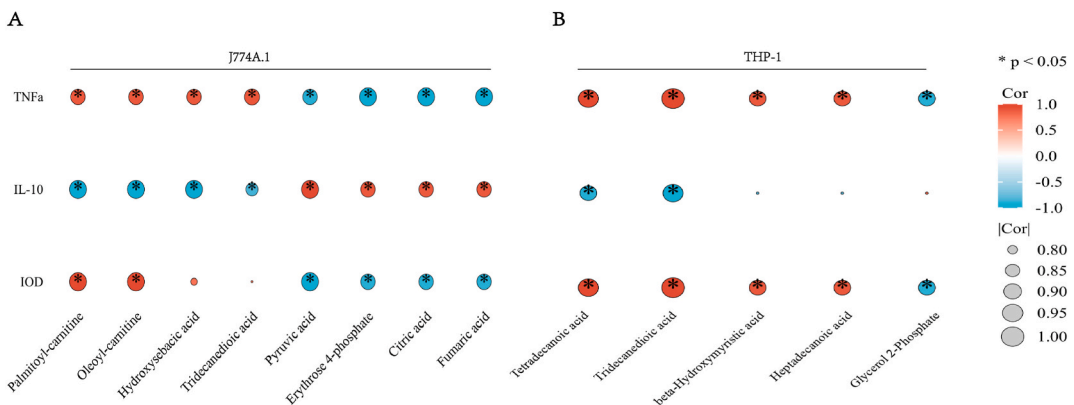


Fig. 9. Correlation analysis of key metabolites with lipid accumulation and cytokines. (A) J774A.1 cell line. (B) THP-1 cell line. *P < 0.05.

2.8. Correlation analysis of key metabolites with lipid accumulation and cytokines

The correlation analysis showed that, in the J774A.1 and THP-1 cells, there was a positive correlation between the fatty acids and their conjugates with TNF- α and IOD, while a negative correlation was observed with IL-10. Conversely, the glucose metabolites showed a positive correlation with IL-10 and a negative correlation with TNF- α and IOD (Fig. 9). However, no correlation was found between key lipid metabolites and cytokines in the BV2 and HMC3 microglia.

3. Discussion

In this study, we investigated the cell viability, lipid uptake, inflammatory gene expression and metabolomics profiles of macrophages and microglia treated with ox-LDL *in vitro*. Our findings indicated that macrophages and microglia display distinct responses to ox-LDL. The ox-LDL enhanced the lipid uptake in both macrophages and microglia, but more accumulated lipids in macrophages than in microglia. Moreover, in macrophages, ox-LDL increased mRNA expression of the pro-inflammatory cytokine TNF- α gene and decreased the mRNA for the anti-inflammatory cytokine IL-10 gene, while there was no difference in cytokine gene expression in microglia. In addition, ox-LDL had varying effects on the dysregulation of lipid, glucose, and amino acid metabolites in macrophages and microglia. Furthermore, fatty acids and their conjugates metabolites showed a positive correlation with TNF- α and a negative correlation with IL-10 in macrophages, but not in microglia.

It has been reported that ox-LDL promotes the transformation of macrophages into foam cells which engage the nuclear factor κ -light-chain-enhancer of activated B cells (NF- κ B) pathway that transcriptionally activates the production of pro-inflammatory cytokines and chemokines to sustain the local inflammatory environment [31–36]. Our findings are consistent with previous research that ox-LDL can lead to lipid accumulation in macrophages and foam cell formation, up-regulation of TNF- α mRNA expression, and down-regulation of IL-10 mRNA expression. This study, for the first time, compared the responses of macrophages and microglia under same ox-LDL concentration. Our data suggested that lipid accumulates in microglia treated with ox-LDL, albeit to a lesser extent than in macrophages. Besides, the changes in cytokine expression were not observed in microglia. These results indicated that ox-LDL-induced local inflammation by macrophages could be a potential cause of the inflammatory damage. This could be explained by a study on age-related macular degeneration [37] that the ox-LDL-induced macrophages and microglia can enhance the apoptosis of retinal pigment epithelium cells. The impact of macrophages on retinal pigment epithelium cell apoptosis after ox-LDL treatment is greater than that of microglia. The variations in the immune responses of macrophages and microglia to ox-LDL suggest that the heterogeneity in cell origin and tissue localization might be critical in influencing the function of immune cells. Macrophages originating from the progenitor cells in the bone marrow are the immune cells widely distributed in the bloodstream and tissues throughout the body [38, 39]. On the other hand, microglia are the resident immune cells present in the central nervous system (CNS) and retina, derived from primitive yolk sac progenitor cells [16,40].

Metabolomics analysis not only reveals different responses of organisms to various microenvironmental perturbations, but also distinguishes the metabolic differences among different individuals of same species. Since ox-LDL influences the function of macrophages and microglia, the cellular metabolism of macrophages and microglia should be altered under ox-LDL treatment. In this study, non-targeted metabolomics approach was used to analyze the changes in metabolites in human and mouse-derived macrophages and microglia under same ox-LDL concentration. In macrophage cell lines, most obvious metabolic effect of the ox-LDL treatment was the up-regulation of fatty acids, especially the oxidized fatty acids, suggesting a potential oxidative stress response in macrophages after the ox-LDL treatment. Lipid aggregation combined with oxidative stress may lead to the formation of lipid peroxidation products and induce the inflammatory response [41]. In this study, we found that, in macrophages (J774A.1 and THP-1 cells), fatty acids and their conjugates were positively correlated with TNF- α and IOD and negatively correlated with IL-10. Carnitine, a fatty acid conjugate, can

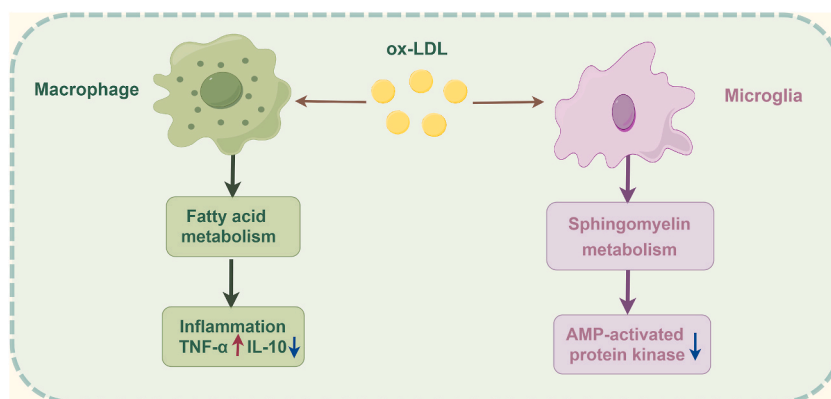


Fig. 10. Schematic representation of the mechanism. Schematic illustration of macrophages and microglia showing different responses to ox-LDL. Ox-LDL induces inflammatory response by enhancing fatty acid metabolism in macrophage. Ox-LDL enhances sphingomyelin metabolism in microglia and may alter AMPK.

facilitate the transport of medium-long chained fatty acids across the outer mitochondrial membrane and undergo β -oxidation to produce acetyl-coA [42]. Inhibition of fatty acid oxidation can enhance the resistance to hypoxia as well as the cardiomyocyte survival and proliferation in adult mice [43]. We therefore speculated that the increased fatty acid oxidation after the ox-LDL treatment in macrophages could inhibit macrophage proliferation. The up-regulation of fatty acid metabolites would induce inflammation, oxidative stress, and mitochondrial dysfunction [44,45]. Unlike macrophages, the primary metabolic change in microglia (BV2 and HMC3) cells after the ox-LDL treatment was the increase in sphingomyelin SM(d18:1/16:0) metabolites. Sphingomyelin SM (d18:1/16:0) plays a role in regulating ATP levels and the AMP-activated protein kinase (AMPK) pathway. AMPK is responsible for maintaining cellular energy balance [46]. The presence of SM(d18:1/16:0) would reduce the AMPK activity, leading to the disruption of cellular energy homeostasis [46].

The accumulation of lipids disrupts the metabolic balance of the cells and causes a decrease in glucose and amino acid metabolism. The glucose metabolism includes glycolysis, the TCA cycle, and the PPP. In this study, we demonstrated that the metabolites involved in glycolysis, the TCA cycle, and the PPP were down-regulated in J774A.1 cells treated with ox-LDL, as compared to the control cells. Previous studies have shown that alterations in the glucose metabolites can affect the macrophage function [47,48]. Macrophages are heterogeneous cell populations that adapt and respond to a variety of microenvironmental stimuli [49]. Depending on the cell surface markers and cytokines release, macrophages are conventionally classified into pro-inflammatory M1 macrophages and anti-inflammatory M2 macrophages [50,51]. Lipopolysaccharide (LPS) induces classical activation of M1 macrophages, whereas IL-4 and IL-13 induce alternative activation program in M2 macrophages [52]. Previous study reported an overall decrease in TCA cycle activity in LPS-activated M1 macrophages [53]. In this study, we showed that the content of TCA cycle metabolites decreased after the ox-LDL treatment in macrophages, indicating that macrophages might convert to M1 after the ox-LDL treatment. We also demonstrated that, in macrophages, glucose metabolites were positively correlated with IL-10 and negatively correlated with TNF- α and IOD, which were related to the inflammatory state of macrophages. Changes in glucose metabolism are accompanied by the alterations in energy levels [27,54]. Creatine, phosphocreatine, ADP, and ATP were all decreased in the four cell lines under the treatment of ox-LDL.

For the amino acid metabolism, both GSH and branched-chain amino acid metabolism were both affected after the ox-LDL treatment. GSH, which is composed of glutamic acid, cysteine and glycine, is the major anti-oxidant in the body and involved in maintaining intracellular redox balance. The decrease in GSH in the ox-LDL-treated J774A.1 and BV2 cells could lead to the reduction of defense against oxidative stress, suggesting that the cells are more prone to oxidative stress after the ox-LDL treatment. Previous studies have demonstrated that dihydromyricetin, xanthoangelol, and isothiocyanates can protect human umbilical vein endothelial cells from inflammatory injury and endothelial dysfunction induced by ox-LDL via increasing GSH [55–57]. The decrease in GSH metabolites suggested that the anti-oxidant defense could be reduced in the J774A.1 and BV2 cells treated with ox-LDL. However, there was no change in GSH in ox-LDL-treated THP-1 cells. On the contrary, glutamate and glycine metabolites, the upstream of GSH, were increased. Their increase might indicate that the THP-1 cells attempt to produce more anti-oxidants to resist oxidative stress following the ox-LDL treatment. Moreover, the metabolism of branched-chain amino acids was also altered in the ox-LDL treated cells. The branched-chain amino acids can be converted into pyruvate for energy generation [58]. The down-regulation of these metabolites might suggest that the cells further experience a decrease in the energy production after the ox-LDL treatment. Compared to the control group, N-acetylalanine was decreased in the J774A.1 cells, but increased in the HMC3 cells. N-acetylalanine can enhance the intracellular anti-oxidant generation and inhibit apoptosis [59]; therefore, under same ox-LDL concentration, the cell viability of J774A.1 cells was decreased, while the cell viability of HMC3 cells remained unchanged. Collectively, our results suggested that ox-LDL mediates the up-regulation of fatty acid metabolites in macrophages, which initiates the inflammatory response, followed by the changes in glucose metabolism and amino acid metabolism to counteract the metabolic instability in the cells. However, ox-LDL mediates the changes in sphingomyelin metabolism in microglia, reduces the AMPK activity, and leads to the dysregulation of cellular energy homeostasis. The heterogeneity of macrophages and microglia in response to the ox-LDL-mediated changes in the microenvironment might explain the inflammatory damage in glaucoma.

There are several limitations in this study. First, cell lines rather than primary cells were used in this study. Limited donor eyes are available for microglia isolation. Second, the results of metabolomics analysis need to be further validated by other experiments. Third, this study was lack of protein expression analysis and animal study. Further investigations are needed to resolve these issues.

In summary, results from this study demonstrated the ox-LDL-mediated changes in the metabolomics profiles of macrophages and microglia that their functional heterogeneity could be related to cell origin and tissue localization, confirming macrophages and microglia as distinct lineages. The extent to which ox-LDL induces lipid loading in macrophages affects inflammatory state. Macrophages may play a role in ox-LDL-induced inflammation in POAG.

4. Materials and methods

4.1. Cell culture

The BV2 murine microglial, J774A.1 murine macrophage, HMC3 human microglial, and THP-1 human monocytic cell lines were purchased from Procell Life Science & Technology Co., Ltd (Procell, Wuhan, China). BV2 and HMC3 cells were cultured in minimum essential medium. J774A.1 cells were cultured in Dulbecco's modified Eagle's medium and THP-1 cells were cultured in RPMI-1640 medium. The media were supplemented with 10% fetal bovine serum and 1% antibiotics. The cells were cultured in an incubator with 5% CO₂ and at 37 °C, and the cells at logarithmic growth phase were taken for the experiments. THP-1 differentiation to macrophages was induced with 200 nM phorbol 12-myristate-13-acetate (PMA; MedChemExpress, Shanghai, China) for 48 h. In the control group, the cells were not treated to the ox-LDL. In the ox-LDL group, the cells were exposed to the ox-LDL. All experiments were performed in

triplicate.

4.2. Preparation of oxidized LDL

Native LDL (Yiyuan Biotechnology Co., Ltd., Guangzhou, China) was oxidized to ox-LDL with 5 μM CuSO_4 for 8 h at 37 $^\circ\text{C}$ as previously described [60]. To terminate the oxidation, 1 mM EDTA (Sangon Biotech Co., Ltd., Shanghai, China) was added, and the degree of oxidation was determined using an MDA assay kit (Beyotime Institute of Biotechnology, Jiangsu, China). The ox-LDL was then dialyzed extensively with phosphate-buffered saline (PBS) to remove the CuSO_4 and concentrated using an ultrafiltration device (Millipore, Billerica, MA). The protein concentration of ox-LDL was quantified with a BCA protein assay kit (Thermo Fischer Scientific, Waltham, MA).

4.3. Cell viability assay

Cell viability was evaluated by the Cell Counting Kit-8 (CCK-8; APEX BIO Technology LLC, Houston, TX). The cells were seeded in 96-well plates at 5×10^3 cells/100 μL /well and incubated with variable concentrations of ox-LDL (0, 6.25, 12.5, 25, 50, and 100 $\mu\text{g}/\text{mL}$) for 0, 24, 48, and 72 h. At each time point, the medium was replaced by a fresh medium containing 10 μL CCK-8 and incubated for 3 h. Absorbance was measured at 540 nm using a microplate reader (BioTek, Winooski, VT).

4.4. Oil red O staining assays

The cells were seeded in 24-well plates at 5×10^4 cells/ml. After ox-LDL treatment, cells were fixed in 4% paraformaldehyde for 15 min. The cells were then washed three times with PBS and placed in propylene glycol for 5 min. The cells were stained with oil red O solution (Abcam, Cambridge, the United Kingdom) for 30 min at room temperature and differentiated in 85% propylene glycol for 1 min. The cells were rinsed twice with distilled water and observed under a light microscope (Leica Microsystems, Wetzlar, Germany). Nine microscopic fields were imaged in each slide. The data were presented as mean intensity (integrated optical density, IOD) using the Image-Pro Plus software.

4.5. DiI-ox-LDL uptake assay

The cells were seeded in 24-well plates at 5×10^4 cells/ml. To assess ox-LDL uptake, cells were incubated with DiI-ox-LDL (Yiyuan Biotechnology Co., Ltd., Guangzhou, China), washed three times with PBS and visualized with an inverted fluorescence microscope (Leica Microsystems).

4.6. Quantitative PCR analysis

The cells were seeded in 24-well plates at 5×10^4 cells/ml. After ox-LDL treatment, total RNAs were extracted using the TRIzol reagent (Thermo Fischer Scientific, Waltham, MA) and reverse transcribed into cDNA according to the RevertAid First Strand cDNA Synthesis Kit (Thermo Fischer Scientific) instructions for subsequent detection by TB Green Premix EX Taq (Tli RNaseH Plus; Takara Biomedical Technology Co. Ltd., Beijing, China) in a real-time PCR machine (Roche, Basel, Switzerland). Primers were shown in table S7.

4.7. Cellular metabolite analysis

The cells were seeded in 60 mm dishes at 1.5×10^5 cells/ml. After ox-LDL treatment, cells were washed twice with PBS and immediately cooled in liquid nitrogen. The cell metabolites were extracted with 1 mL 80% (v/v) methanol and collected for the untargeted metabolomics analysis by the liquid chromatography–mass spectrometry (LC-MS) platform (Waters, UPLC; Thermo, Q Exactive). The LC-MS was performed using a Waters ACQUITY UPLC HSS T3 (2.1 mm \times 100 mm 1.8 μm columns) using the following chromatographic separation conditions: column temperature at 40 $^\circ\text{C}$; flow rate at 0.3 mL/min; mobile phase A as water (0.05% ammonium); mobile phase B as acetonitrile; injection volume of 5 μL ; automatic injector temperature at 4 $^\circ\text{C}$. The gradient elution procedures are described in table S6.

4.8. LC-MS data collection and analysis

Raw data obtained by the LC-MS was imported into Compound Discoverer 3.1 software, and data quality control was carried out. The data was subjected to the multivariate statistical analysis, using unsupervised principal component analysis (PCA) and orthogonal projections to latent structures-discriminant analysis (OPLS-DA) to evaluate the whole clustering trends and visualize the distributions. The quality of the models was evaluated with the relevant R^2Y and Q^2 . The differentially abundance metabolites were screened based on criteria of a variable importance in the projection (VIP) > 1 and $P < 0.05$.

4.9. Statistical analysis

Data were presented as mean of 3 repeated experiments \pm standard deviations (SD). SPSS 27.0 software (SPSS, Chicago, IL) was used to perform independent T-test to compare two groups. $P < 0.05$ was considered as statistically significant. GraphPad Prism 7.0 (GraphPad Software Inc., San Diego, CA, USA) was used for graphing.

Funding statement

This research was funded by National Natural Science Foundation of China (grant number: 82,171,044), Special Fund for Science and Technology of Guangdong Province (grant number: 2019ST024), and Natural Science Foundation of Guangdong Province (grant number: 2022A1515011646).

Data availability statement

The data in this study did not deposit into a publicly available repository and are available upon request from the corresponding authors.

Ethical approval

Ethical approval is not required in this study.

Institutional review board statement

Not applicable.

Informed consent statement

Not applicable.

CRediT authorship contribution statement

Yaru Sun: Writing – original draft, Methodology, Formal analysis, Data curation. **Jia-Jian Liang:** Methodology, Conceptualization. **Jianming Xu:** Formal analysis. **Kewen Zhou:** Formal analysis. **Changzhen Fu:** Methodology. **Shao-Lang Chen:** Methodology. **Rucui Yang:** Methodology. **Tsz Kin Ng:** Writing – review & editing. **Qingping Liu:** Writing – review & editing, Supervision, Funding acquisition, Conceptualization. **Mingzhi Zhang:** Writing – review & editing, Supervision, Funding acquisition, Conceptualization.

Declaration of competing interest

The authors declare that they have no known competing financial interests or personal relationships that could have appeared to influence the work reported in this paper.

Acknowledgments

Figs. 7, 8 and 10 was drawn by Figdraw (www.figdraw.com).

Appendix A. Supplementary data

Supplementary data to this article can be found online at <https://doi.org/10.1016/j.heliyon.2024.e28806>.

References

- [1] Y.-C. Tham, X. Li, T.Y. Wong, H.A. Quigley, T. Aung, C.-Y. Cheng, Global prevalence of glaucoma and projections of glaucoma burden through 2040 : a systematic review and meta-analysis, *Ophthalmology* 121 (2014) 2081–2090, <https://doi.org/10.1016/j.ophtha.2014.05.013>.
- [2] R.N. Weinreb, P.T. Khaw, Primary open-angle glaucoma, *Lancet* 363 (2004) 1711–1720, [https://doi.org/10.1016/s0140-6736\(04\)16257-0](https://doi.org/10.1016/s0140-6736(04)16257-0).
- [3] H.L. Zeng, J.M. Shi, The role of microglia in the progression of glaucomatous neurodegeneration- a review, *Int. J. Ophthalmol.* 11 (2018) 143–149, <https://doi.org/10.18240/ijo.2018.01.22>.
- [4] P.A. Williams, C.E. Braine, K. Kizhatil, N.E. Foxworth, N.G. Tolman, J.M. Harder, R.A. Scott, G.L. Sousa, A. Panitch, G.R. Howell, et al., Inhibition of monocyte-like cell extravasation protects from neurodegeneration in DBA/2J glaucoma, *Mol. Neurodegener.* 14 (2019) 6, <https://doi.org/10.1186/s13024-018-0303-3>.
- [5] G.R. Howell, I. Soto, X. Zhu, M. Ryan, D.G. Macalinao, G.L. Sousa, L.B. Caddle, K.H. MacNicoll, J.M. Barbay, V. Porciatti, et al., Radiation treatment inhibits monocyte entry into the optic nerve head and prevents neuronal damage in a mouse model of glaucoma, *J. Clin. Invest.* 122 (2012) 1246–1261, <https://doi.org/10.1172/jci61135>.

- [6] G. Thorleifsson, G.B. Walters, A.W. Hewitt, G. Masson, A. Helgason, A. DeWan, A. Sigurdsson, A. Jonasdottir, S.A. Gudjonsson, K.P. Magnusson, et al., Common variants near CAV1 and CAV2 are associated with primary open-angle glaucoma, *Nat. Genet.* 42 (2010) 906–909, <https://doi.org/10.1038/ng.661>.
- [7] Z. Wu, C. Huang, Y. Zheng, X.L. Yuan, S. Chen, Y. Xu, L.J. Chen, C.P. Pang, M. Zhang, T.K. Ng, Primary open-angle glaucoma risk prediction with ABCA1 and LOC102723944 variants and their genotype-phenotype correlations in southern Chinese population, *Mol. Genet. Genom.* : MGG 298 (2023) 1343–1352, <https://doi.org/10.1007/s00438-023-02058-6>.
- [8] M. Modrzejewska, W. Grzesiak, D. Zaborski, A. Modrzejewska, The role of lipid dysregulation and vascular risk factors in glaucomatous retrobulbar circulation, *Bosn. J. Basic Med. Sci.* 15 (2015) 50–56, <https://doi.org/10.17305/bjbm.2015.299>.
- [9] R.S. Joshi, V.H. Adatiya, Study of the relationship between serum lipid levels and primary open-angle glaucoma, *Indian J. Ophthalmol.* 71 (2023) 1948–1952, https://doi.org/10.4103/ijo.ijo_3233_22.
- [10] M.J. Kim, M.J. Kim, H.S. Kim, J.W. Jeoung, K.H. Park, Risk factors for open-angle glaucoma with normal baseline intraocular pressure in a young population: the Korea National Health and Nutrition Examination Survey, *Clin. Exp. Ophthalmol.* 42 (2014) 825–832, <https://doi.org/10.1111/ceo.12347>.
- [11] M. Helin-Toiviainen, S. Rönkkö, K. Kaamiranta, T. Puustjärvi, P. Rekonen, M. Ollikainen, H. Uusitalo, Oxidized low-density lipoprotein, lipid and calcium aggregates reveal oxidative stress and inflammation in the conjunctiva of glaucoma patients, *Acta Ophthalmol.* 95 (2017) 378–385, <https://doi.org/10.1111/aos.13380>.
- [12] R. Yang, Q. Liu, M. Zhang, The past and present lives of the intraocular transmembrane protein CD36, *Cells* 12 (2022), <https://doi.org/10.3390/cells12010171>.
- [13] Y. Chen, J. Zhang, CD36, a signaling receptor and fatty acid transporter that regulates immune cell metabolism and fate, *J. Exp. Med.* 219 (2022), <https://doi.org/10.1084/jem.20211314>.
- [14] S. Li, J.M. Navia-Pelaez, S.H. Choi, Y.I. Miller, Macrophage inflammarrafts in atherosclerosis, *Curr. Opin. Lipidol.* 34 (2023) 189–195, <https://doi.org/10.1097/mol.0000000000000888>.
- [15] M. Locati, G. Curtale, A. Mantovani, Diversity, mechanisms, and significance of macrophage plasticity, *Annual review of pathology* 15 (2020) 123–147, <https://doi.org/10.1146/annurev-pathmechdis-012418-012718>.
- [16] C. Yu, C. Roubeix, F. Sennlaub, D.R. Saban, Microglia versus monocytes: distinct roles in degenerative diseases of the retina, *Trends Neurosci.* 43 (2020) 433–449, <https://doi.org/10.1016/j.tins.2020.03.012>.
- [17] H. Wu, M. Wang, X. Li, Y. Shao, The metaflammatory and immunometabolic role of macrophages and microglia in diabetic retinopathy, *Hum. Cell* 34 (2021) 1617–1628, <https://doi.org/10.1007/s13577-021-00580-6>.
- [18] E.L. Fletcher, Contribution of microglia and monocytes to the development and progression of age related macular degeneration, *Ophthalmic Physiol. Opt.* : the journal of the British College of Ophthalmic Opticians (Optometrists) 40 (2020) 128–139, <https://doi.org/10.1111/opo.12671>.
- [19] P.A. Williams, C.E. Braine, K. Kizhatil, N.E. Foxworth, N.G. Tolman, J.M. Harder, R.A. Scott, G.L. Sousa, A. Panitch, G.R. Howell, et al., Inhibition of monocyte-like cell extravasation protects from neurodegeneration in DBA/2J glaucoma, *Mol. Neurodegener.* 14 (2019), <https://doi.org/10.1186/s13024-018-0303-3>.
- [20] M.A. Margeta, E.M. Lad, A.D. Proia, CD163+ macrophages infiltrate axon bundles of postmortem optic nerves with glaucoma, *Graefes Arch. Clin. Exp. Ophthalmol.* 256 (2018) 2449–2456, <https://doi.org/10.1007/s00417-018-4081-y>.
- [21] D.X. Hammer, A. Agrawal, Label-free adaptive optics imaging of human retinal macrophage distribution and dynamics, *Proc. Natl. Acad. Sci. U.S.A.* 117 (2020) 30661–30669, <https://doi.org/10.1073/pnas.2010943117>.
- [22] F. Alliot, I. Godin, B. Pessac, Microglia derive from progenitors, originating from the yolk sac, and which proliferate in the brain, *Brain research. Developmental brain research* 117 (1999) 145–152, [https://doi.org/10.1016/s0165-3806\(99\)00113-3](https://doi.org/10.1016/s0165-3806(99)00113-3).
- [23] C.H. Alves, R. Fernandes, A.R. Santiago, Microglia contribution to the regulation of the retinal and choroidal vasculature in age-related macular degeneration, *Cells* 9 (2020), <https://doi.org/10.3390/cells9051217>.
- [24] P.A. Williams, N. Marsh-Armstrong, G.R. Howell, Neuroinflammation in glaucoma: a new opportunity, *Exp. Eye Res.* 157 (2017) 20–27, <https://doi.org/10.1016/j.exer.2017.02.014>.
- [25] A. Zhang, H. Sun, H. Xu, S. Qiu, X. Wang, Cell metabolomics, *OMICS A J. Integr. Biol.* 17 (2013) 495–501, <https://doi.org/10.1089/omi.2012.0090>.
- [26] M. Ambeskovic, G. Hopkins, T. Hoover, J.T. Joseph, T. Montina, Metabolomic signatures of alzheimer's disease indicate brain region-specific neurodegenerative progression, *Int. J. Mol. Sci.* 24 (2023), <https://doi.org/10.3390/ijms241914769>.
- [27] A. Alamri, L. Biswas, Deletion of TSPO resulted in change of metabolomic profile in retinal pigment epithelial cells, *Int. J. Mol. Sci.* 20 (2019), <https://doi.org/10.3390/ijms20061387>.
- [28] G.L. Seim, E.C. Britt, S.V. John, F.J. Yeo, A.R. Johnson, R.S. Eisenstein, D.J. Pagliarini, J. Fan, Two-stage metabolic remodelling in macrophages in response to lipopolysaccharide and interferon- γ stimulation, *Nat. Metab.* 1 (2019) 731–742, <https://doi.org/10.1038/s42255-019-0083-2>.
- [29] V.L. Nelson, H.C.B. Nguyen, J.C. Garcia-Cañaveras, E.R. Briggs, W.Y. Ho, J.R. DiSpirito, J.M. Marinis, D.A. Hill, M.A. Lazar, PPAR γ is a nexus controlling alternative activation of macrophages via glutamine metabolism, *Gene Dev.* 32 (2018) 1035–1044, <https://doi.org/10.1101/gad.312355.118>.
- [30] G. Luo, X. Wang, Y. Cui, Y. Cao, Z. Zhao, J. Zhang, Metabolic reprogramming mediates hippocampal microglial M1 polarization in response to surgical trauma causing perioperative neurocognitive disorders, *J. Neuroinflammation* 18 (2021) 267, <https://doi.org/10.1186/s12974-021-02318-5>.
- [31] D.A. Chistiakov, A.A. Melnichenko, V.A. Myasoedova, A.V. Grechko, A.N. Orekhov, Mechanisms of foam cell formation in atherosclerosis, *J. Mol. Med.* 95 (2017) 1153–1165, <https://doi.org/10.1007/s00109-017-1575-8>.
- [32] R.J. Lightbody, J.M.W. Taylor, Y. Dempsey, A. Graham, MicroRNA sequences modulating inflammation and lipid accumulation in macrophage "foam" cells: implications for atherosclerosis, *World J. Cardiol.* 12 (2020) 303–333, <https://doi.org/10.4330/wjc.v12.i7.303>.
- [33] A. Sato, H. Unuma, K. Ebina, Royal jelly proteins inhibit macrophage proliferation: interactions with native- and oxidized-low density lipoprotein, *Protein J.* 40 (2021) 699–708, <https://doi.org/10.1007/s10930-021-09998-1>.
- [34] B. Ye, X. Liang, Y. Zhao, X. Cai, Z. Wang, S. Lin, W. Huang, P. Shan, W. Huang, Z. Huang, Hsa_circ_0007478 aggravates NLRP3 inflammasome activation and lipid metabolism imbalance in ox-LDL-stimulated macrophage via miR-765/EFNA3 axis, *Chem. Biol. Interact.* 368 (2022) 110195, <https://doi.org/10.1016/j.cbi.2022.110195>.
- [35] D. Karunakaran, M.A. Nguyen, M. Geoffrion, D. Vreeken, Z. Lister, H.S. Cheng, N. Otte, P. Essebier, H. Wyatt, J.W. Kandiah, et al., RIPK1 expression associates with inflammation in early atherosclerosis in humans and can be therapeutically silenced to reduce NF- κ B activation and atherogenesis in mice, *Circulation* 143 (2021) 163–177, <https://doi.org/10.1161/circulationaha.118.038379>.
- [36] L. He, X. Zhao, L. He, LINC01140 alleviates the oxidized low-density lipoprotein-induced inflammatory response in macrophages via suppressing miR-23b, *Inflammation* 43 (2020) 66–73, <https://doi.org/10.1007/s10753-019-01094-y>.
- [37] G. Devarajan, J. Niven, J.V. Forrester, I.J. Crane, Retinal pigment epithelial cell apoptosis is influenced by a combination of macrophages and soluble mediators present in age-related macular degeneration, *Curr. Eye Res.* 41 (2016) 1235–1244, <https://doi.org/10.3109/02713683.2015.1109129>.
- [38] S. Epelman, K.J. Lavine, G.J. Randolph, Origin and functions of tissue macrophages, *Immunity* 41 (2014) 21–35, <https://doi.org/10.1016/j.immuni.2014.06.013>.
- [39] T.A. Wynn, A. Chawla, J.W. Pollard, Macrophage biology in development, homeostasis and disease, *Nature* 496 (2013) 445–455, <https://doi.org/10.1038/nature12034>.
- [40] E.G. O'Koren, C. Yu, M. Klingeborn, A.Y.W. Wong, C.L. Prigge, R. Mathew, J. Kalnitsky, R.A. Msallam, A. Silvin, J.N. Kay, et al., Microglial function is distinct in different anatomical locations during retinal homeostasis and degeneration, *Immunity* 50 (2019) 723–737.e727, <https://doi.org/10.1016/j.immuni.2019.02.007>.
- [41] E. Kaemmerer, F. Schutt, T.U. Krohne, F.G. Holz, J. Kopitz, Effects of lipid peroxidation-related protein modifications on RPE lysosomal functions and POS phagocytosis, *Invest. Ophthalmol. Vis. Sci.* 48 (2007) 1342–1347, <https://doi.org/10.1167/iov.06-0549>.
- [42] M.S. Trabjerg, D.C. Andersen, P. Huntjens, K.E. Oklinski, L. Bolther, J.L. Hald, A.E. Baisgaard, K. Mørk, N. Warming, U.B. Kullab, et al., Downregulating carnitine palmitoyl transferase 1 affects disease progression in the SOD1 G93A mouse model of ALS 4 (2021) 509, <https://doi.org/10.1038/s42003-021-02034-z>.

- [43] X. Li, F. Wu, S. Guenther, M. Looso, C. Kuenne, T. Zhang, M. Wiesnet, S. Klatt, S. Zukunft, I. Fleming, et al., Inhibition of fatty acid oxidation enables heart regeneration in adult mice, *Nature* 622 (2023) 619, <https://doi.org/10.1038/s41586-023-06585-5>.
- [44] L.P. Shriver, M. Manchester, Inhibition of fatty acid metabolism ameliorates disease activity in an animal model of multiple sclerosis, *Sci. Rep.* 1 (2011) 79, <https://doi.org/10.1038/srep00079>.
- [45] G.J. van der Windt, B. Everts, C.H. Chang, J.D. Curtis, T.C. Freitas, E. Amiel, E.J. Pearce, E.L. Pearce, Mitochondrial respiratory capacity is a critical regulator of CD8+ T cell memory development, *Immunity* 36 (2012) 68–78, <https://doi.org/10.1016/j.immuni.2011.12.007>.
- [46] S. Miyamoto, C.C. Hsu, G. Hamm, M. Darshi, M. Diamond-Stanic, A.E. Declèves, L. Slater, S. Pennathur, J. Stauber, P.C. Dorresteine, et al., Mass spectrometry imaging reveals elevated glomerular ATP/AMP in diabetes/obesity and identifies sphingomyelin as a possible mediator, *EBioMedicine* 7 (2016) 121–134, <https://doi.org/10.1016/j.ebiom.2016.03.033>.
- [47] R.P. Brandes, F. Rezende, Glycolysis and inflammation: partners in crime, *Circ. Res.* 129 (2021) 30–32, <https://doi.org/10.1161/circresaha.121.319447>.
- [48] B. Kelly, L.A. O'Neill, Metabolic reprogramming in macrophages and dendritic cells in innate immunity, *Cell Res.* 25 (2015) 771–784, <https://doi.org/10.1038/cr.2015.68>.
- [49] L. Zhu, Q. Zhao, T. Yang, W. Ding, Y. Zhao, Cellular metabolism and macrophage functional polarization, *Int. Rev. Immunol.* 34 (2015) 82–100, <https://doi.org/10.3109/08830185.2014.969421>.
- [50] Y. Yao, X.H. Xu, L. Jin, Macrophage polarization in physiological and pathological pregnancy, *Front. Immunol.* 10 (2019) 792, <https://doi.org/10.3389/fimmu.2019.00792>.
- [51] Q. Zhang, J. Wang, D.K. Yadav, X. Bai, T. Liang, Glucose metabolism: the metabolic signature of tumor associated macrophage, *Front. Immunol.* 12 (2021) 702580, <https://doi.org/10.3389/fimmu.2021.702580>.
- [52] S.J. Van Dyken, R.M. Locksley, Interleukin-4- and interleukin-13-mediated alternatively activated macrophages: roles in homeostasis and disease, *Annu. Rev. Immunol.* 31 (2013) 317–343, <https://doi.org/10.1146/annurev-immunol-032712-095906>.
- [53] G.M. Tannahill, A.M. Curtis, J. Adamik, E.M. Palsson-McDermott, A.F. McGettrick, G. Goel, C. Frezza, N.J. Bernard, B. Kelly, N.H. Foley, et al., Succinate is an inflammatory signal that induces IL-1 β through HIF-1 α , *Nature* 496 (2013) 238–242, <https://doi.org/10.1038/nature11986>.
- [54] D.G. Ryan, L.A.J. O'Neill, Krebs cycle reborn in macrophage immunometabolism, *Annu. Rev. Immunol.* 38 (2020) 289–313, <https://doi.org/10.1146/annurev-immunol-081619-104850>.
- [55] Y. Luo, S. Lu, X. Dong, L. Xu, G. Sun, X. Sun, Dihydromyricetin protects human umbilical vein endothelial cells from injury through ERK and Akt mediated Nrf2/HO-1 signaling pathway, *Apoptosis: an international journal on programmed cell death* 22 (2017) 1013–1024, <https://doi.org/10.1007/s10495-017-1381-3>.
- [56] R. Yan, J. Yan, X. Chen, Y. Yu, T. Sun, Xanthoangelol prevents ox-LDL-induced endothelial cell injury by activating Nrf2/ARE signaling, *J. Cardiovasc. Pharmacol.* 74 (2019) 162–171, <https://doi.org/10.1097/fjc.0000000000000699>.
- [57] C.S. Huang, A.H. Lin, C.T. Liu, C.W. Tsai, I.S. Chang, H.W. Chen, C.K. Lii, Isothiocyanates protect against oxidized LDL-induced endothelial dysfunction by upregulating Nrf2-dependent antioxidation and suppressing NF κ B activation, *Mol. Nutr. Food Res.* 57 (2013) 1918–1930, <https://doi.org/10.1002/mnfr.201300063>.
- [58] H. Takagi, Metabolic regulatory mechanisms and physiological roles of functional amino acids and their applications in yeast, *Biosci. Biotechnol. Biochem.* 83 (2019) 1449–1462, <https://doi.org/10.1080/09168451.2019.1576500>.
- [59] G.A. Cunningham, N.H. McClenaghan, P.R. Flatt, P.L. Newsholme, Alanine induces changes in metabolic and signal transduction gene expression in a clonal rat pancreatic beta-cell line and protects from pro-inflammatory cytokine-induced apoptosis, *Clinical science (London, England : 1979)* 109 (2005) 447–455, <https://doi.org/10.1042/cs20050149>.
- [60] Q. Liu, K. Kobayashi, J. Furukawa, J. Inagaki, N. Sakairi, A. Iwado, T. Yasuda, T. Koike, D.R. Voelker, E. Matsuura, Omega-carboxyl variants of 7-ketocholesterol esters are ligands for beta(2)-glycoprotein I and mediate antibody-dependent uptake of oxidized LDL by macrophages, *J. Lipid Res.* 43 (2002) 1486–1495, <https://doi.org/10.1194/jlr.m20063-jlr200>.